· Article ·
doi: 10.13679/j.advps.2014.1.00001

Advances in Polar Science
March 2014 Vol. 25 No. 1: 1-9

Thickness distribution and extent of sea ice and snow in Prydz Bay and surrounding waters observed in 2012/2013 austral summer

CHENG Peng[1*], HAN Hongwei[1], LEI Ruibo[2], LI Zhijun[1] & LU Peng[1]

[1] State Key Laboratory of Coastal and Offshore Engineering, Dalian University of Technology, Dalian 116024, China;
[2] Polar Research Institute of China, Shanghai 200136, China

Received 30 July 2013; accepted 22 January 2014

Abstract Three ship-based observational campaigns were conducted to survey sea ice and snow in Prydz Bay and the surrounding waters (64.40°S–69.40°S, 76.11°E–81.29°E) from 28 November 2012 to 3 February 2013. In this paper, we present the sea ice extent and its variation, and the ice and snow thickness distributions and their variations with time in the observed zone. In the pack ice zone, the southern edge of the pack ice changed little, whereas the northern edge retreated significantly during the two earlier observation periods. Compared with the pack ice, the fast ice exhibited a significantly slower variation in extent with its northernmost edge retreating southwards by 6.7 km at a rate of 0.37 km·d^{-1}. Generally, ice showed an increment in thickness with increasing latitude from the end of November to the middle of December. Ice and snow thickness followed an approximate normal distribution during the two earlier observations (79.7±28.9 cm, 79.1±19.1 cm for ice thickness, and 11.6±6.1 cm, 9.6±3.4 cm for snow thickness, respectively), and the distribution tended to be more concentrated in mid-December than in late November. The expected value of ice thickness decreased by 0.6 cm, whereas that of snow thickness decreased by 2 cm from 28 November to 18 December 2012. Ice thickness distribution showed no obvious regularity between 31 January and 3 February, 2013.

Keywords **sea ice, snow, thickness, summer, Prydz Bay**

Citation: Cheng P, Han H W, Lei R B, et al. Thickness distribution and extent of sea ice and snow in Prydz Bay and surrounding waters observed in 2012/2013 austral summer. Adv Polar Sci, 2014, 25: 1-9, doi: 10.13679/j.advps.2014.1.00001

1 Introduction

Antarctica is the cold source of the global atmosphere. As a key factor of Antarctica, sea ice plays an important role in global climate processes[1-3]. It prevents the direct exchange of heat flow between the atmosphere and ocean by both increasing surface albedo and insulating the relatively warm ocean from the atmosphere in winter. Heat flux in the pack ice zone is complex because of the wide difference in albedos between open water, snow, and sea ice[4] and because of the thermodynamic interactions between the pack ice and leads[5]. What's more, wave-ice interaction has become the focus of research on sea ice dynamics because it is the most recurrent environmental influence of the marginal ice zone[6-7]. To obtain a better understanding of all the processes mentioned above, it is necessary to establish basic information regarding sea ice, e.g., sea ice extent and its variation, and snow and ice thicknesses and their distributions.

Several methods have been applied to survey the thickness and extent of sea ice in Antarctica. Satellite remote sensing is an effective tool for assessing large-scale ice cover[8-9], rapidly obtaining large amounts of sea ice data. However, some limitations should be taken into consideration. For example, satellite sensors have low spatial resolution when distinguishing water from sea ice. Furthermore, the reliability of ice thicknesses determined by satellite altimeters depends on the accuracy of the snow depth data set and the

*Corresponding author (email: chengpeng0710@gmail.com)

densities of the snow and ice[10-11]. In addition, satellite-derived ice concentrations could cause errors when dealing with high or low concentrations of sea ice[12]. In situ measurement is another method for acquiring basic parameters of sea ice and snow in Antarctica. Although it can provide an accurate data set, the amount of information recorded from ground-based observations is generally poor in the region of interest because of the adverse climatic environment[13]. Owing to their mobility, ship-based observations[14-15] provide a larger survey platform than ground-based observations. Compared with satellite remote sensing, they have higher spatial resolution and provide relatively reliable results. Thus, it is preferential that satellite remote sensing results should be combined with ship-based observations to evaluate sea ice and snow in Antarctica.

As part of the 29th Chinese National Antarctic Research Expedition, ship-based observations were conducted to survey the sea ice and snow in Prydz Bay and the surrounding waters. In this paper, we present details of the sea ice extent and its variation, and the ice and snow thickness distributions and their variations with time in the observed zone.

2 Observations

2.1 Study area and cruise tracks

Both the thickness and the extent of sea ice in Prydz Bay and the surrounding waters change seasonally. In winter, Prydz Bay and the surrounding waters are covered completely by sea ice, which can be up to 2-m thick[16]. In summer, most sea ice in this region melts, although some, particularly near the coast, survives throughout the summer. We conducted three ship-based observational campaigns from 28 November 2012 to 3 February 2013 in the study area (64.40°S–69.40°S, 76.11°E–81.29°E). Figure 1 shows the study area and the three tracks of the R/ V *XUE LONG* icebreaker. The start and end dates of each track are indicated in Table 1. The three observational campaigns lasted five, three and four days, respectively.

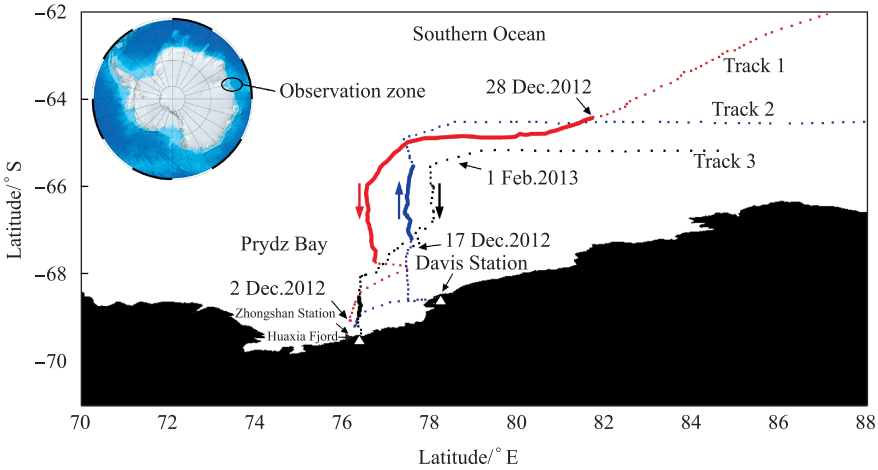

Figure 1 Map of the three cruise tracks of the R/V *XUE LONG* icebreaker. The colored arrows indicate the cruise directions of each track of the same color. The solid line of each track illustrates the pack ice zone and the dotted line represents the open water zone. Further details of each track are presented in Table 1.

2.2 Observation method

We used a ship-based downward-looking video camera for the measurement of sea ice and snow thickness[17-18]. When the icebreaker broke the sea ice, the cross section of the sea ice plate and snow appeared above the water and it was captured by the video camera. A 30-cm-diameter buoy was hung above the horizontal plane as a scale calibration. The camera and buoy were set at positions about 7 and 0.5 m above the water, respectively. A GPS device was used to record positional information. By comparing pixels of the ice and snow section with the buoy diameter, we can obtain ice and snow thicknesses along the ship tracks. Two digital cameras were fixed to the top of ship, one on each side, in an outward-facing orientation. Thus, sea ice conditions over a large area around the ship can be captured and used to estimate the sea ice extent[13,19]. Ship-based ASPeCt observations were conducted every 30 min to estimate ice concentration within an area with a 1-km radius. In addition, we measured the fast ice thickness by drilling holes in Huaxia Fjord near the Zhongshan Station on 11 December 2012; a location that the R/V *XUE LONG* icebreaker was unable to reach because of thick fast ice. The mean diameter of the calibration buoy in the video was 54 pixels, which give a resolution of 0.56 cm per pixel. The pixels of the cross section of the sea ice and snow were measured manually using image processing software. This caused errors of no more than 4 pixels, which gave an accuracy of ±2.22 cm. Camera optic axis deviation from the vertical direction caused by the ship's sway was another source of error. According to photogrammetric theory, deviations of 5°, 10°, and 15° theoretically cause a relative error of 0.38%, 1.52%, and 3.41%, respectively.

3 Results

3.1 Sea ice extent

Table 1 presents the details of the sea ice extent observed during the cruise tracks of the three observational campaigns. The R/V *XUE LONG* icebreaker cruised along Track 1 to Zhongshan Station from November 28, reaching the position 69.21°S, 76.12°E on December 2, a point about 20 km from Zhongshan Station. The most northerly pack ice observed along the track was at 61.60°S, 87.60°E. A little pack ice was found scattered between 61.60°S and 64.40°S; the ice concentration in these latitudes was so low, mostly below 30%, that as the R/V *XUE LONG* icebreaker voyaged through the leads, no ice or snow cross sections were captured by the video camera[17]. In this paper, we focus attention on the areas of high ice concentration. The pack ice concentration between 64.40°S and 67.67°S was sufficiently high, mostly above 70%, to be captured by the video camera. We found an area of open water between 67.67°S and 69.04°S, which was almost completely free of ice. Fast ice covered the zone south of 69.04°S to the coast near Zhongshan Station. The R/V *XUE LONG* icebreaker cruised northwards along Track 2, away from Zhongshan Station on 15 December 2012. Because it turned to the east at 64.50°S, 78.53°E, we were unable to observe the northernmost pack ice position. During this time, the open water extent became greater than in the first period (Table 1). The earlier observed pack ice extent narrowed, becoming distributed between the latitudes of 65.50°S–67.17°S. However, the northern part of the fast ice observed earlier had melted and a new pack ice zone (68.89°S–69.10°S) had emerged. By the time of Track 3, the fast ice had dissolved totally. The coastal zone was free of ice and only a little pack ice was found between 68.50°S and 68.90°S.

Table 1 Sea ice range during each track

Track No.	Date (Year/Month/Day)	Pack ice extent	Open water extent	Fast ice extent
1	2012/11/28–2012/12/2	64.40°S–67.67°S	67.67°S–69.04°S	69.04°S–coast
2	2012/12/15–2012/12/18	65.50°S–67.17°S 68.89°S–69.10°S	67.17°S–68.89°S	69.10°S–coast
3	2013/1/31–2013/2/3	68.50°S–68.90°S	68.90°S–coast	—

Because ship-based observations can only observe ice along the cruise track, we present remotely sensed images of sea ice extent and concentration in Prydz Bay in Figure 2. The first and second observations were conducted in the Antarctic midsummer with intense solar radiation, and the sea ice extent changed drastically during this period. According to the data recorded by the meteorological station onboard the R/V *XUE LONG* icebreaker, the daily mean air temperatures and wind speeds from 27 November to 29 November when the R/V *XUE LONG* icebreaker cruised south through the pack ice zone were −0.6, −1.7, and −2.8℃ and 27.3, 15.6, and 7.5 $m \cdot s^{-1}$, respectively. When the R/V *XUE LONG* icebreaker moved north through the pack ice zone from 17 December to 18 December, the daily mean air temperatures and wind speeds were 1.2 and −1.1℃ and 3.2 and 6.0 $m \cdot s^{-1}$, respectively. During the first observation, the northern edge of the pack ice in the study area was between 63.50°S and 64.40°S and the southern edge was between 66.50°S and 67.20°S. Compared with the first observations, the southern edge of the pack ice during the second observational period changed little, whereas the northern edge exhibited significant retreat. Wind-generated waves can break pack ice into smaller pieces and a rise of air temperature can contribute to the ice melting. As a supplement, sea ice drift may also play a role in the retreat of the northern edge of the pack ice. The Antarctic Divergence near Prydz Bay and the surrounding waters is generally between 65°S–66°S[20]. The northern part of the pack ice was located north of the Antarctic Divergence, where the mean current was to the east. Mean ocean circulation can cause sea ice drift over long time scales, but a drastic decline in ice extent within a short period may also be influenced by synoptic factors, for example, sea ice drift driven by wind. Despite the enlargement of the open-water area in the south of the pack ice over a long time scale, the southern edge of the pack ice may move southwards in a short time, causing a decrease in the open-water area. This phenomenon can be found by comparing the southern edge of the pack ice in Figures 2c and 2d. Ice melt in the inner part of the pack ice zone was slower, because of the relatively calm environment. Ice concentration was lower at the edge of the pack ice zone than in the inner part, as demonstrated in Figure 2. The northern edge of the fast ice retreated by only 6.7 km, which indicates a decay rate of 0.37 $km \cdot d^{-1}$. Compared with the pack ice in the same sector, the fast ice in the higher-latitude zone was thicker and suffered less environmental impact, which lead to a significantly slower variation in extent and much longer melting period.

3.2 Ice thickness distribution

We obtained 481, 588, and 29 ice thickness values via the ship-based video camera method during the three observational campaigns, respectively. We also obtained 23 ice thickness values in Huaxia Fjord by drilling holes, covering the latitude range of 64.40°S–69.40°S. In addition, 77 and 56 values of ice concentration from the pack ice zone were recorded during the first and second observational campaigns, respectively. Most thickness values of the two

earlier observational campaigns were obtained from the fast ice zone, while the third observational campaign contained only values of pack ice thickness. Thicknesses were divided into groups according to ice condition and the number of thickness samples at different latitudes. The means and standard deviations of the ice thicknesses in each group were determined. Figure 3 presents the ice thickness variation with latitude, in which a, b, and c represent the three tracks shown in Table 1. Figure 4 presents the pack ice concentration with latitude during the first and second observational campaigns.

Generally, ice showed an increment in thickness with increasing latitude from the end of November to the middle of December. In the pack ice zone, ice thickness did not increase directly with latitude, but it fluctuated. In Figure 3a, the mean values of ice thickness on the edge of the pack ice zone (64.40°S–64.60°S, 67.67°S) were 38 and 18 cm, respectively. These are much smaller than in the inner part, where the values ranged from 42 to 77 cm. This was attributed to the open water. On the one hand, water without ice cover tends to form waves more easily under the action

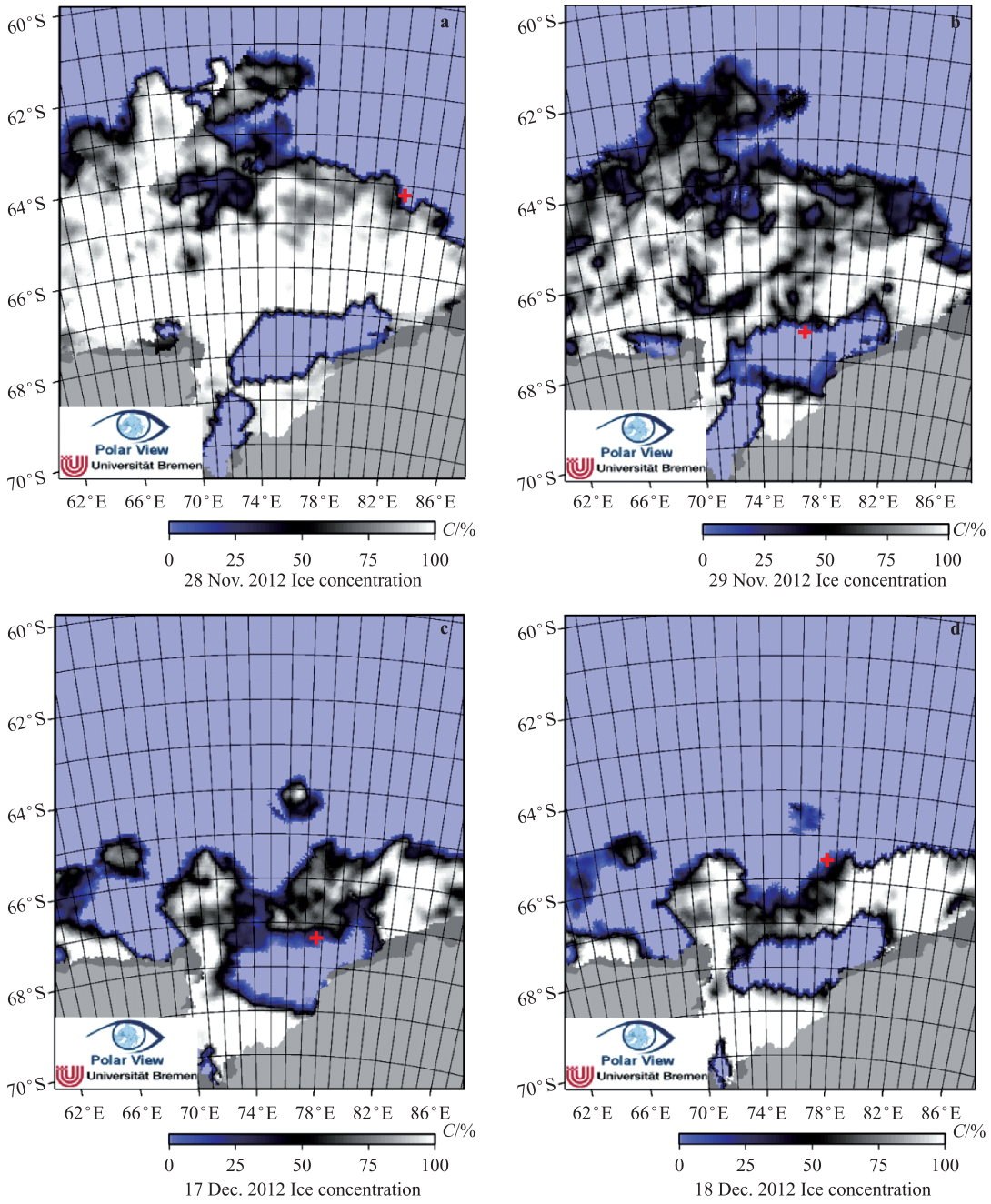

Figure 2 Concentration and extent of sea ice in Prydz Bay derived from SSMIS. Red cross marks the location where the R/V *XUE LONG* icebreaker entered and left the pack ice zone. **a**, **b** and **c**, **d** were during the first and second observational campaign, respectively. SSMIS data were provided by the University of Bremen.

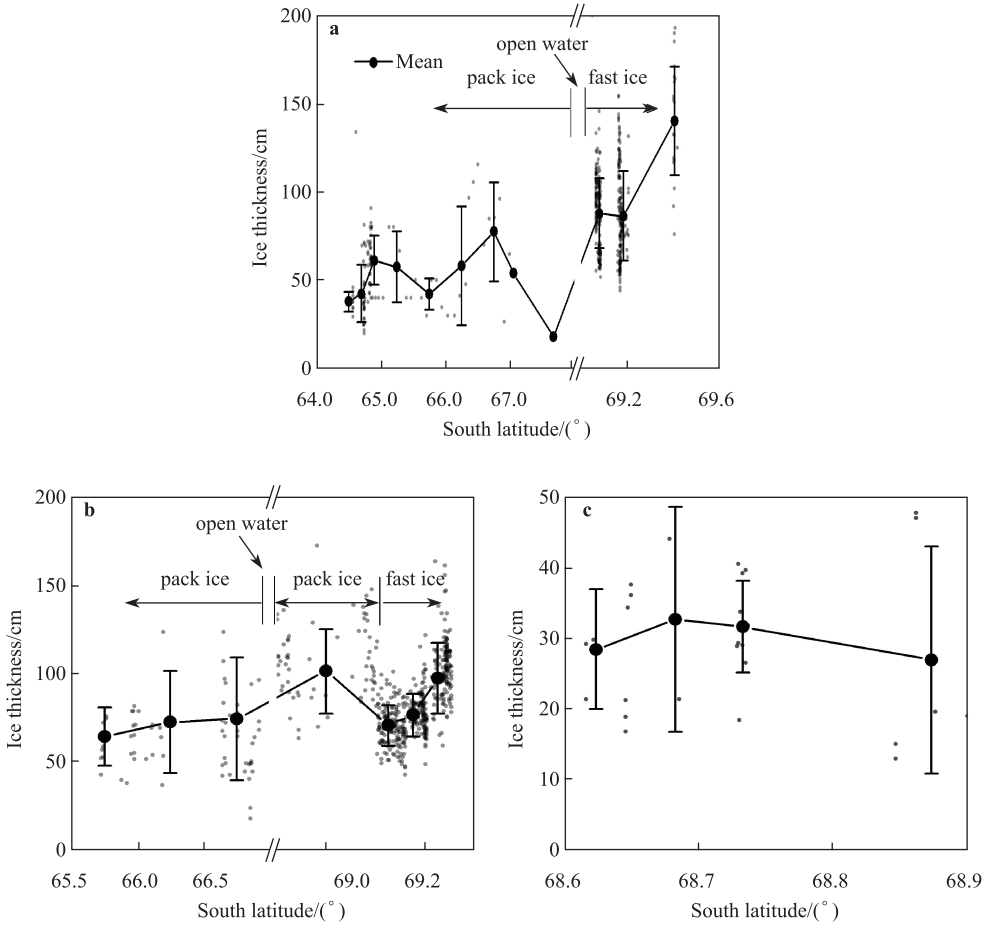

Figure 3 Variation of ice thickness with latitude. **a**, **b**, and **c** represent the three observational campaigns presented in Table 1. Note the gap in the horizontal axes of both **a** and **b** where ice thickness values were not available because of open water. Furthermore, note that there are only mean values from 67°S to 68°S in **a** because only two thickness values were obtained. **a**, the values at 69.40°S were measured in Huaxia Fjord by drilling holes, as mentioned above.

of wind, promoting the breaking up and melting of the pack ice. On the other hand, water absorbs more heat from solar radiation than ice and snow do; thus, the heat flow in the horizontal direction is enhanced, which results in significant lateral melting of the pack ice. Therefore, ice concentration at the edge of the pack ice zone was lower than that in the inner part (Figure 4). In Figure 3b, the extent of the pack ice can be seen to be narrower than that shown in Figure 3a. Pack ice thickness tends to be uniform; the mean value between 65.50°S and 66.50°S was around 65 cm, which is greater than the thicknesses of 42 and 58 cm at the same latitudes in Figure 3a. The thickness distribution of Antarctic pack ice is determined by both thermodynamic and dynamic processes[21]. Sea ice drift physically redistributes the pack ice and changes its extent and concentration. Through deformations, such as rafting, piling up, and ridge building, the distribution of ice thickness is changed[22]. Furthermore, the cruise tracks of the observational campaigns cannot coincide exactly, which is why greater ice thicknesses were found in the pack ice zone at some latitudes during the second observational campaign than in the first. In Figure 3c, pack ice thickness is shown to have changed little with latitude; the mean values are around 30 cm.

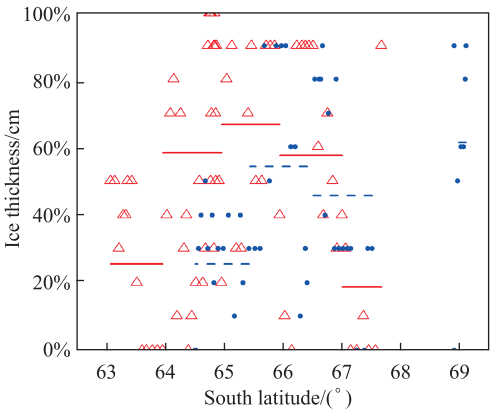

Figure 4 Pack ice concentration derived from ASPeCt observations on the first and second tracks. Triangles and solid dots represent observed values of the first and second observational campaigns, respectively. The solid and dashed lines represent their mean values.

In contrast to the pack ice, ice thickness in the fast ice zone increased obviously with decreasing distance to the coast, which can be established from the mean values. The mean value of fast ice thickness on the outer part of the fast ice zone (69.10°S) in Figure 3a was 88 cm. However, the value obtained by drilling holes in Huaxia Fjord (69.40°S) near the coast, increased rapidly to 140 cm. The same regularity can be found in Figure 3b. Ice in the inner part of the fast ice zone, taking Huaxia Fjord as an example, was thicker than in the outer part, which was caused by the geomorphology. Many small islands are scattered in the coastal area off Zhongshan Station, and a large number of icebergs become grounded in this area, making it a place that suffers little from dynamic action. Thus, the growth and degradation of sea ice near the coast is almost entirely determined by thermodynamic process[23], and the sea ice there is thicker than further offshore. We discovered that the mean values decreased by about 10 cm, when comparing the fast ice thicknesses in Figure 3b with the ice thicknesses at similar latitudes (69.15°S–69.20°S) in Figure 3a; the thickness variation over time in the fast ice zone was slow.

Standard deviations of pack ice thickness in Figure 3 show no obvious regularity with latitude. The standard deviations in Figure 3a range from 5.4 to 33.8 cm, which is attributed to the small number of ice thickness samples captured by the video camera in the pack ice zone, randomness of ice monitoring by video camera, and the complex ocean dynamic and thermodynamic environment of the area. In contrast to the pack ice, the dispersion degree of fast ice thicknesses increases with increasing latitude (Figures 3a and 3b), leading to larger standard deviations.

Figure 5 demonstrates the frequency distributions of ice thicknesses in the first two observational campaigns, μ represents the expected value of thickness, i.e., abscissa values of the peak on curve; σ represents mean square deviation. The probabilities of ice thickness distributed within the range of $\mu\pm\sigma$ in Figures 5a and 5b are 0.690 and 0.641, respectively, while that of the standard normal distribution is similar at 0.683. Ice thickness followed an approximate normal distribution in the period between late November (Figure 5a) and mid-December (Figure 5b). Two peaks of 65 and 90 cm are found in Figure 5a. However, in Figure 5b, it changes to a unimodal distribution with a maximum of 75 cm. The expected value (μ) changes little between the two earlier observations, but the mean square deviation (σ) decreases by about 10 cm. In Figure 5b, the proportion of ice thinner than 10 cm and thicker than 120 cm decreases compared with Figure 5a, whereas it increases for ice thickness between 60 and 120 cm. Young ice, which is generally thin and located in the pack ice zone, melts quickly. The decrease of thick ice occurs in the fast ice zone and thus, ice thickness distribution tends to be more concentrated and homogeneous in mid-December (79.1±19.1 cm) than it is in late November (79.7±28.9 cm). During the third observational campaign, the sea ice was in the final phase of the melting period and only 29 pack ice thicknesses were obtained between 68.50°S and 68.90°S. This sample size is too small to represent the real situation accurately and therefore, the statistical parameters of μ and σ were ignored. As a comparison, the mean value of the 29 thicknesses from the third cruise was 29.5 cm, which is much smaller than that determined from the two earlier observational campaigns.

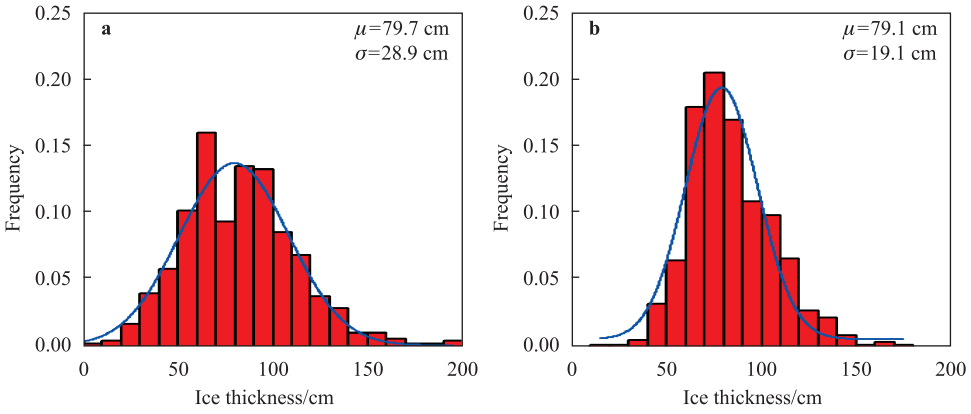

Figure 5 Frequency distributions of ice thicknesses. **a** and **b** represent the first and second observational campaigns presented in Table 1, respectively, including both pack ice and fast ice. The binning increments are both 10 cm. Unimodal lines represent the fitted normal distribution curves.

3.3 Snow thickness distribution

We obtained 226 and 409 snow thickness values by ship-based methods during the first two observational campaigns, respectively. Snow thickness values were not acquired during the third cruise because sea ice concentration during this time was low and the snow thicknesses were so thin that it could not be recognized by the video camera. Figure 6 presents the snow thickness variation with latitude, which is quite different to that of the ice. Ice thickness shows a huge difference between the pack ice and fast ice, whereas snow thickness shows no obvious difference between them. The mean value of the variation of snow thickness with latitude is insignificant; the ranges of variation in Figures 6a and

6b are 5.5–15.2 cm and 10.5–22.2 cm, respectively, with a maximum extent of 11.7 cm. In the pack ice zone, snow at the same latitude (65.0°S–67.0°S) during the second cruise was thicker than that in the first, similar to the ice thickness mentioned in section 3.2. Because snow exists on top of the sea ice, movement of sea ice causes the redistribution of snow thickness to some degree. Furthermore, persistently strong winds over the Antarctic sea ice, typically observed following precipitation events, is another key element of snow thickness distribution[23-24]. The redistribution of dry unconsolidated snow is initiated at wind speeds in excess of 6–8 $m \cdot s^{-1}$[25]. As an addition, slush generated by rain and melted snow refreezes into ice, reducing the snow thickness[26]. Despite the unimpressive distribution of mean snow thickness with latitude, the mean snow thickness reaches a peak in the highest latitude of the fast ice zone in Figure 6; the latitude at which the ice was relatively thick. Mean snow thickness decreases by about 4.7 cm in Figure 6b compared with Figure 6a at similar latitude (69.10°S–69.20°S) in the fast ice zone. The standard deviation of snow thickness has a similar variation trend as the mean value (Figure 6), i.e., the area with thicker snow generally has a greater dispersion degree of snow thickness, and vice versa.

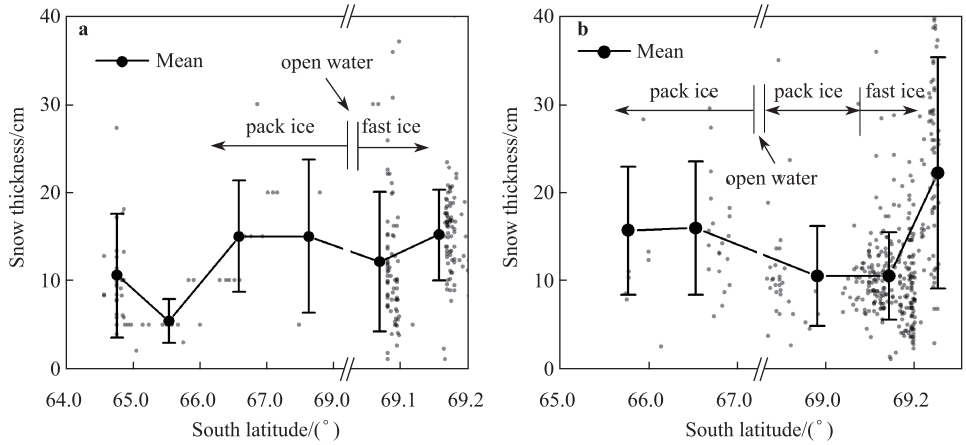

Figure 6 Variation of snow thickness with latitude. **a** and **b** represent the first and second observational campaigns presented in Table 1, respectively. Note the gap in the horizontal axes where snow thickness was not available because of open water.

Figure 7 demonstrates the frequency distributions of snow thicknesses in the two earlier cruises. Snow thicknesses follow an approximate normal distribution, but tailing slightly to the right; thus, the fitted normal distribution curves are unsymmetrical in Figure 7, which is different to the curve of ice thickness distribution in Figure 5. Therefore, there is a much greater probability of snow that is thinner than the mid-value of thickness than thicker. Multiple peaks are found around μ and $\mu \pm \sigma$ in Figure 7a because the snow thickness distribution was scattered during the first cruise. Similar to the distribution of ice thickness in Figure 5b, there is only one peak within the range of $\mu \pm \sigma$ in Figure 7b. The variation of snow thickness distribution in Figure 7 can be explained by the decreasing proportion of snow that is thinner than 6 cm and between 14 and 20 cm. Similar to the variation of ice thickness distribution in Figure 5, the snow thickness values

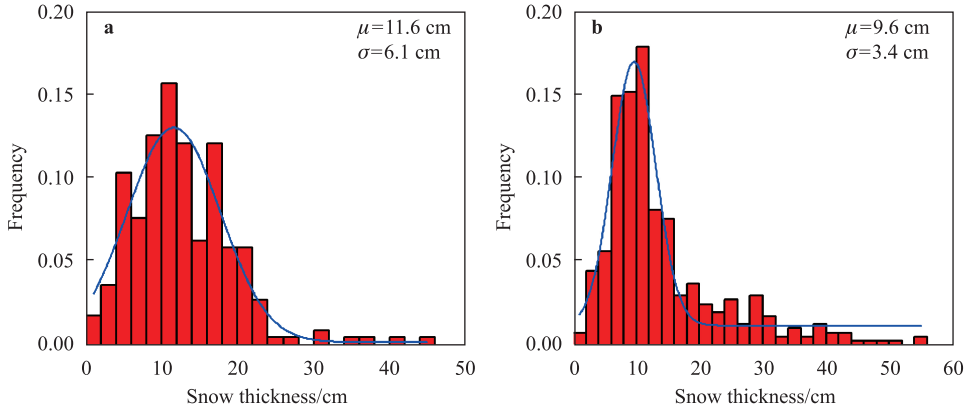

Figure 7 Frequency distributions of snow thicknesses. **a** and **b** represent the first and second observational campaigns presented in Table 1, respectively. The binning increments are 2 cm. Unimodal lines represent the fitted normal distribution curves; μ and σ represent the expected value and mean square deviation of snow, respectively, as defined in Figure 5.

in Figure 7b are more concentrated than in Figure 7a, mostly distributed over the range of 9.6±3.4 cm. An interesting and unusual fact is that the proportion of snow between 25 and 35 cm increases, rather than decreases. This could be interpreted as follows. We observed snow in a higher-latitude zone (69.25°S) during the second observational campaign (Figure 6b) than during the first (Figure 6a); the mean value of snow thickness in the higher-latitude zone was 22.2 cm, which is larger than any other observed zone. By comparing the expected value (μ) of snow and ice thickness during the two earlier cruises, it can be seen that the former decreases by 2 cm, whereas the latter almost retains the same value. As mentioned above, the mean thickness of ice in latitudes 69.15°S–69.20°S, decreased by about 10 cm, whereas that of snow in similar latitudes of 69.10°S–69.20°S decreased by 4.7 cm. Considering that the mean thickness of ice is about 5–7 times larger than that of snow in those latitudes, we conclude that snow is more sensitive to environmental change than ice is.

4 Conclusions

We conducted three ship-based observational campaigns to survey the sea ice and snow in Prydz Bay and the surrounding waters (64.40°S–69.40°S, 76.11°E–81.29°E) during the period 18 November 2012 to 3 February 2013. A wide open-water zone was found between the pack ice zone and fast ice zone in Prydz Bay during the end of November and middle of December 2012, the position of which changed with time. Distribution ranges of pack ice varied under the impact of dynamic and thermodynamic factors; the southern edge of the pack ice changed little, whereas the northern edge retreated significantly. Fast ice showed a significantly slower variation in extent with a mean decay rate of 0.37 $km \cdot d^{-1}$. The third cruise was conducted at the end of January and in early February 2013, at which time the pack ice was distributed only within 68.50°S–68.90°S, whereas the fast ice had melted completely.

Generally, sea ice showed an increment in thickness with increasing latitude, especially in the fast ice zone, from the end of November to mid-December. Both the northern and southern parts of the pack ice zone adjoined open water, which made the ice thinner at those points than in the middle part. Ice concentration at the edge of the pack ice zone was lower than that in the inner part. Ice thickness followed an approximate normal distribution during the two earlier cruises. The expected value of ice changed little between the first two observational periods, but the mean square deviation decreased by 10 cm. Ice thickness distribution tended to be more concentrated and homogeneous during the middle of December (79.1±19.1 cm) than at the end of November (79.7±28.9 cm).

The variation of the mean value of snow thickness with latitude is unimpressive; however, the thickest snow was found in the highest latitude of the fast ice zone. Snow thickness followed an approximate normal distribution. The expected value of snow thickness during mid-December is 2 cm less than that between 28 November and 2 December 2012. The snow thickness frequency distribution exhibited multiple peaks at the end of November, which turned into a single-peak distribution and tended to be more concentrated and homogeneous by the middle of December, similar to that found for the ice distribution.

Acknowledgments This work is supported by the Foundation for Innovative Research Groups of the National Natural Science Foundation of China (Grant no. 51221961), the National Basic Research Program of China (Grant no. 2010 CB950301), and the International Science and Technology Cooperation Project (Grant no. 2011DFA22260). The fieldwork was performed during the 29th Chinese National Antarctic Research Expedition organized by the Chinese Arctic and Antarctic Administration. Data were issued by the Data-sharing Platform of Polar Science (http://www.chinare.org.cn) maintained by Polar Research Institute of China (PRIC) and Chinese National Arctic & Antarctic Data Center (CN-NADC). We thank the PRIC for providing excellent logistic support.

References

1 Haskell T. What's so important about sea ice. Water Atmos, 2003, 11(3): 28-29.
2 Walsh J E. The role of sea ice in climate variability: theories and evidence. Atmos -Ocean, 1983, 21(3): 229-242.
3 Hanna E. The role of Antarctic sea ice in global climate change. Prog Phys Geogr, 1996, 20(4): 371-401.
4 Allison I, Brandt R E, Warren S G. East Antarctic sea ice: albedo, thickness distribution, and snow cover. J Geophys Res, 1993, 98(C7): 12417-12429.
5 Lei R B, Li Z J, Cheng B, et al. Investigation of the thermodynamic processes of a floe-lead system in the central Arctic during later summer. Adv Polar Sci, 2011, 22(1): 10-16.
6 Lu P, Li Z J, Zhang Z H, et al. Aerial observations of floe size distribution in the marginal ice zone of summer Prydz Bay. J Geophys Res, 2008, 113, C02011, doi:10.1029/2006JC003965.
7 Meylanl M H, Masson D. A linear Boltzmann equation to model wave scattering in the marginal ice zone. Ocean Modell, 2006, 11(3-4): 417-427.
8 Worby A P, Comiso J C. Studies of the Antarctic sea ice edge and ice extent from satellite and ship observations. Remote Sens Environ, 2004, 92(1): 98-111.
9 Worby A P, Steer A, Lieser J L, et al. Regional-scale sea-ice and snow thickness distributions from in situ and satellite measurements over East Antarctica during SIPEX 2007. Deep-Sea Res II, 2011, 58(9-10): 1125-1136.
10 Kurtz N T, Markus T, Cavalieri D J, et al. Estimation of sea ice thickness distributions through the combination of snow depth and satellite laser altimetry data. J Geophys Res, 2009, 114, C10007, doi:10.1029/2009JC005292.
11 Maksym T, Markus T. Antarctic sea ice thickness and snow-to-ice conversion from atmospheric reanalysis and passive microwave snow depth. J Geophys Res, 2008, 113, C02S12, doi:10.1029/2006JC004085.
12 Lu P, Li Z J, Cheng B, et al. Sea ice surface features in Arctic summer 2008: Aerial observations. Remote Sens Enviro, 2010, 114(4): 693-699.
13 Richard J H, Nick H, Peter W. A systematic method of obtaining ice concentration measurements from ship-based observations. Cold

Regions Sci Technol, 2002, 34(2): 97-102.
14 Shotaro U, Haruhito S, Koh I. Ship-based sea ice observations in Lützow-Holm Bay, east Antarctica//Proceedings of the 16th IAHR International Symposium on Ice. Dunedin, New Zealand, 2002: 218-224.
15 Niioka T, Cho K. Sea ice thickness measurement from an ice breaker using a stereo imaging system consisted of a pairs of high definition video cameras. Int Arch Photogram, Remote Sens Spatial Infor Sci, 2010, 38(8): 1053-1056.
16 Pu S Z, Dong Z Q. Progress in physical oceanographic studies of Prydz Bay and its adjacent oceanic area. Chin J Polar Res, 2003, 15(1): 53-64 (in Chinese).
17 Cho K, Taniguchi Y, Nakayama M, et al. Sea ice thickness measurement using stereo image // The 17th International Symposium on Okhotsk Sea & Sea Ice. Hokkaido, Japan, 2002: 169-172.
18 Lei R B, Cheng Y F, Guo J X. Exploration of using digitalized image method base on CCD for sea ice investigation in Bohai Sea. Marine Forecasts, 2008, 25(4): 71-77 (in Chinese).
19 Lu P, Li Z J. A method of obtaining ice concentration and floe size from shipboard oblique sea ice images. IEEE Trans Geosc Remote Sens, 2010, 48(7): 2771-2780.
20 Le K T, Shi J X, Yu K L, et al. Some thoughts on the spatiotemporal variations of water masses and circulations in the region of Prydz Bay, Antarctica. Studia Mar Sin, 1998, 40: 43-54 (in Chinese).
21 Worby A P, Massom R A, Allison I, et al. East Antarctic sea ice: A review of its structure, properties and drift//Jeffries M O. Antarctic Sea Ice: Physical Processes, Interactions and Variability. Washington, DC: American Geophysical Union, 2013, doi: 10.1029/AR074p0041.
22 Heil P, Allison I. The pattern and variability of Antarctic sea-ice drift in the Indian Ocean and western Pacific sectors. J Geophys Res, 1999, 104(C7): 15789-15802.
23 Massom R A, Lytle V I, Worby A P, et al. Winter snow cover variability on East Antarctic sea ice. J Geophys Res, 1998, 103(C11): 24837-24855.
24 Massom R A, Drinkwater M R, Haas C. Winter snow cover on sea ice in the Weddell Sea. J Geophys Res, 1997, 102(C1): 1101-1117.
25 Andreas E L, Claffey K J. Air-ice drag coefficients in the western Weddell Sea: 1. Values deduced from profile measurements. J Geophys Res, 1995, 100(C3): 4821-4831.
26 Fichefet T, Morales Maqueda M A. Modelling the influence of snow accumulation and snow-ice formation on the seasonal cycle of the Antarctic sea-ice cover. Climate Dyn, 1999, 15(4): 251-268.